BL11XU
QST Quantum Dynamics I

1. Abstract

BL11XU is an in-vacuum undulator beamline operated by the National Institutes for Quantum and Radiological Science and Technology (QST). It is designed to provide scientists and engineers with a wide range of options on advanced synchrotron radiation and quantum functional material research. In this beamline, switchable Si(111) and Si(311) double-crystal monochromators cooled by liquid nitrogen are installed in the optical hutch. Highly brilliant and directional synchrotron X-rays are available in the energy range of 6–70 keV. There are three experimental hutches; each one contains specialized measurement instruments for studies using Mössbauer spectroscopy (EH1), inelastic X-ray scattering and X-ray magnetic circularly polarized emission (EH2), and surface X-ray diffraction (EH3).

2.Mössbauer spectroscopy

The study of the surface/interface magnetism of 3*d* transition metals is of interest owing to the essential role that magnetism plays in determining the magnetic interactions of functional nanomagnets. Over the past few decades, various methods have advanced the study of surface/interface magnetism. However, few experimental studies have focused on the depth-dependent surface magnetism at the atomic layer level.

The surface magnetism of iron is a fascinating research subject for atomic-layer-resolved analysis. Theoretical studies predict a 30% enhancement of the magnetic moment M_{Fe} at the surface and an oscillatory behavior with increasing depth in individual layers, *i.e.*, magnetic Friedel oscillation [1]. As a related phenomenon, Ohnishi et al. theoretically predicted that the hyperfine field H_{int} is reduced by 30% relative to the bulk value despite a marked increase in the surface M_{Fe} [2].

Recently, we have determined the layer-by-layer H_{int} of the Fe(001) surface by the in situ ^{57}Fe probe layer method with a high-brilliance synchrotron Mössbauer source [3]. In this method, a resonant isotope probe layer is embedded in a thin film prepared with a non-resonant isotope. The observed H_{int} at the nucleus provides details on the local surface magnetism.

Fe(001) films were fabricated by alternatively evaporating ^{56}Fe and ^{57}Fe from 99.94% ^{56}Fe and 95.93% ^{57}Fe isotopic sources onto pre-cleaned 10×10×0.5 mm^3 MgO(001) substrates under a vacuum pressure of approximately 10^{-8} Pa. A 0.8-ML-thick ^{57}Fe probe layer (t = 0.1 nm) was embedded to the depth of the N^{th} atomic layer below the surface where N = 1 to 4 and 7. These samples are hereafter referred to as "N^{th} probe layer samples".

The experiments were performed at BL11XU of SPring-8 using linearly π-polarized 14.4 keV Mössbauer γ-rays of 15.4 neV bandwidth produced by a synchrotron Mössbauer source. The γ-ray beam was vertically focused by an elliptical mirror. The beam size was 15 μm (V) × 1.6 mm (H) and the beam flux was ~ 2.9×10^4 photons/s. The beam was introduced into the measurement

chamber to perform grazing incidence measurements (Fig. 1(a)). An external field of 300 Oe was applied antiparallel to the beam direction to magnetize the film. In this optics, the π-polarized incident beam interacted with the four nuclear transitions of $\Delta m = \pm 1$. The Mössbauer absorption spectra were measured by collecting the totally reflected γ-rays from the sample surface at an incident angle of 0.1° with a reflectivity of approximately 80%. Each spectrum was obtained within 3 hours of sample preparation. Such rapid measurements reduced the residual gas absorption and oxidation on the Fe(001) surfaces.

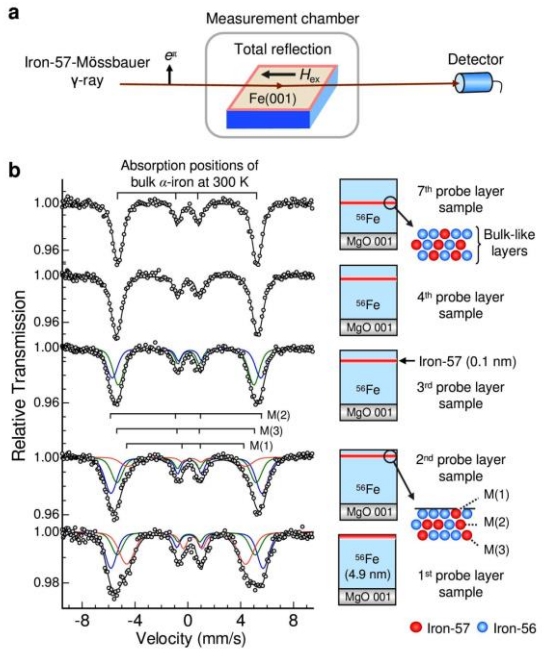

Fig. 1. (a) Experimental setup. (b) Mössbauer spectra of N^{th} probe layer samples measured at 300K. Black solid lines represent the fitted curves. Red, blue, and green lines represent the three different magnetic components. M(i) represents the magnetic component assigned to the ^{57}Fe atoms located in the i^{th} layer below the surface. H_{ex} is the magnetic field (300 Oe).

Figure 1(b) shows the Mössbauer spectra of the N^{th} probe layer samples (N = 1 to 4 and 7) recorded at 300 K. All samples showed magnetically split Mössbauer patterns. The spectra of the 1st, 2nd, and 3rd probe layer samples exhibited complex profiles composed of different magnetic components, i.e., small H_{int} (red lines, around 28 T), large H_{int} (blue lines, around 36 T), and bulk-like H_{int} (green lines, around 32 T).

The ideal probe layer in the sample was surrounded by finely distributed ^{57}Fe atoms, which stemmed from the random deposition and surface diffusion of iron atoms during the growth process. Figure 1(b) (right) shows a conceptual diagramof the process. In this case, if the 1st, 2nd, and 3rd layers of the iron surface have a different H_{int}, the spectra should exhibit a complex profile with multiple components. As shown by the systematic behaviors of the three components, the small H_{int}, large H_{int}, and bulk-like H_{int} represent the intrinsic hyperfine fields for the 1st, 2nd, and 3rd layers from the surface, respectively. In contrast, the spectra of the 4th and 7th probe layer samples exhibited a single magnetic component with four absorption lines, even in the presence of finely distributed ^{57}Fe atoms. This is because the hyperfine fields of the neighboring layers at these depths are bulk-like, and the overlapping subspectra result in a simple absorption profile. The prominent subspectrum with the largest percent area in the N^{th} probe layer sample was assigned to the spectrum characterizing the ^{57}Fe atoms located in the N^{th} atomic layer from the surface.

The experimentally determined layer-by-layer H_{int} exhibited a marked decrease at the surface and an oscillatory decay toward the bulk value. Such a behavior was well reproduced

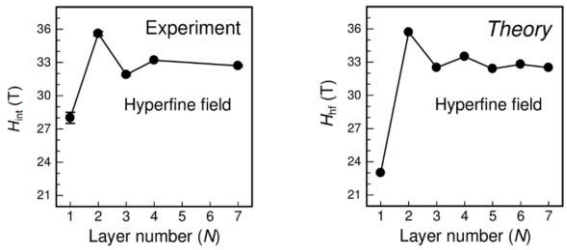

Fig. 2. Experimental and theoretical layer-by-layer hyperfine fields.

by theoretical calculations (Fig. 2). This result provides the first experimental evidence for the magnetic Friedel oscillations, which penetrate several layers below the Fe(001) surface. Theoretically, the oscillatory decay of H_{int} should be strongly coupled with the Friedel oscillation of M_{Fe}, which is caused by the surface electronic structure with a large spin imbalance and *d*-band narrowing [1–3].

In summary, the surface magnetism of Fe(001) was studied in an atomic layer-by-layer manner by using the in situ ^{57}Fe probe layer method with a synchrotron Mössbauer source. The observed H_{int} exhibited a marked decrease at the surface and an oscillatory behavior with increasing depth in the individual upper four layers below the surface. In the future, the in situ ^{57}Fe probe layer method with a synchrotron Mössbauer source should facilitate additional studies on the surface and interface magnetism in advanced magnetic and spintronic materials and devices.

3. Inelastic X-ray scattering

An inelastic X-ray scattering spectrometer for hard X-rays installed in EH2 is mostly used for resonant inelastic X-ray scattering (RIXS) at the *K*-edge of the 3*d* transition metals and the *L*-edge of the 5*d* transition metals as well as X-ray emission spectroscopy.

Recently, 5*d* transition-metal compounds have received considerable attention in condensed matter physics owing to their novel electronic states generated by the interplay between on-site Coulomb repulsion and strong spin-orbit coupling. RIXS at the *L*-edge is a suitable technique for determining the 5*d* electronic states through the observation of *dd* excitations. Spherical analyzers for the L_3-edge of Ta, W, Re, Ir, and Pt and the L_2-edge of Ir have been prepared, and the experimentally achieved energy resolution at respective edges is summarized in Table 1. An energy resolution higher than 150 meV is available for the 5*d* transition metals except for Os. By the *L*-edge RIXS technique, a semimetallic electronic structure formed by spin-orbit coupling was examined in $Li_3Ir_3O_8$ [4].

On the other hand, RIXS at the *K*-edge is sensitive to charge excitations, and it has been applied to the study of single-crystalline

Table 1.L absorption edges of 5d transition metal, Bragg reflection of analyzer crystal, and experimentally achieved energy resolution.

Element	Edge	Energy at absorption edge (eV)	Reflection of analyzer	Achieved resolution (meV)
Ta	L_3	9881	Ge(840)	82
W	L_3	10207	Si(555)	150
Re	L_3	10535	Si(911)	120
Os	L_3	10871	N/A	-
Ir	L_3	11215	Si(844)	43
	L_2	12824	Si(775)	150
Pt	L_3	11564	Si(755)	130

electron-doped cuprates [5], where both element substitution for electron doping and post-growth annealing are indispensable for the occurrence of superconductivity. The charge excitation spectra indicate that electrons are doped in the annealed state even in the unsubstituted Nd_2CuO_4, whereas a clear charge-transfer gap is observed in the as-grown state. Superconductivity in unsubstituted single crystals can potentially be realized, as has already been reported in thin films and polycrystalline samples.

The spectrometer has also been used for the Kβ emission spectroscopy of the iron pnictide superconductors $NaFe_{1-x}Co_xAs$ and $NaFe_{1-x}Cu_xAs$ [6]. As NaFeAs is doped with Co, the local magnetic moment of Fe is slightly reduced, whereas Cu doping leaves it unaffected, implying a different doping mechanism, even though the doping of both Co and Cu induces superconductivity.

4. X-ray magnetic circularly polarized emission

X-ray magnetic circularly polarized emission (XMCPE) is a phenomenon in which characteristic X-rays emitted from a magnetized sample are circularly polarized. XMCPE was reported as a new magneto-optical effect in the X-ray region in 2017 [7]. An advantage of XMCPE is the large flipping ratio (>20%) in the hard X-ray region for 3*d* transition metal elements. This feature is well suited for observations of magnetic microstructures well below the surface of iron- and cobalt-rich ferromagnetic materials.

Accordingly, a bulk-sensitive magnetic microscope utilizing XMCPE schematically shown in Fig. 3 has been developed and installed at BL11XU in FY2018 and FY2019. The crucial elements of the microscope are (i) focusing optics, (ii) collimating optics, and (iii) circular polarization analyzer. The focusing optics focuses incident X-rays onto a sample using a compound refractive lens. There are two lenses for 17.3 keV and 26 keV. The focal spot size of the lenses is about 10 μm. The collimating optics transforms divergent characteristic X-rays emitted from the sample into a well-collimated beam using a laterally graded multilayer Montel mirror. The multilayer period is tuned for 6.4 keV (Fe Kα emission). The circular polarization analyzer measures the degree of circular polarization of the characteristic X-rays and consists of a phase plate (diamond 220) and a linear polarization analyzer (Ge 440). The magnetization of the emitting area is then evaluated from the observed degree of circular polarization. A magnetization image is obtained by scanning a sample. Mainly, magnetic microstructures of electrical steel sheets have been observed as the main target of this project.

In FY2020, the following four experiments were performed.

(a) The beam divergence after the collimating mirror, XMCPE spectra, and magnetization images of a grain-oriented electrical steel sheet were

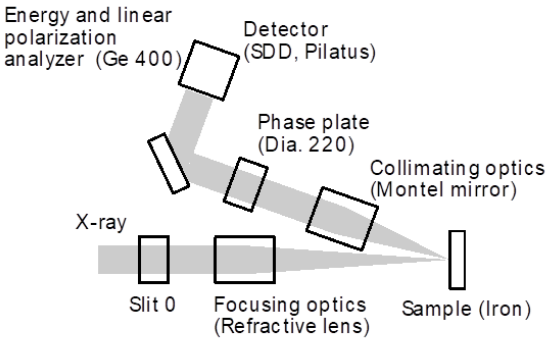

Fig. 3. Schematic of XMCPE microscope in BL11XU.

measured under the same condition for publication [8].

(b) New large diamond phase plates (6 mm × 6 mm × 0.5 mm and 6 mm × 6 mm × 0.3 mm) were examined.

(c) The development of magnetic domains was observed as a function of magnetic fields from the saturated state to the fully reversed state. The sample was a grain-oriented electrical steel sheet. Magnetization images of 10 μm lateral resolution were observed at the beginning of the magnetization reversal, near the demagnetization state, and just before the complete magnetization reversal.

(d) A test of a depth-resolved measurement was carried out using a grain-oriented electrical steel sheet. Judging from the obtained data, it seems that a depth-resolved measurement is possible in XMCPE microscopy. However, it also seems that particular care is necessary for quantitative evaluation.

5. Surface X-ray diffraction

EH3 is equipped with a surface X-ray diffractometer connected with a molecular beam epitaxy (MBE) chamber [9,10]. This instrument is designed for *in situ* studies on III–V group semiconductor surfaces, especially surface crystallography under MBE conditions and growth dynamics of multilayers and nanostructures. III–V group semiconductors are nitrides such as GaN and InN and arsenides such as GaAs and InAs. These semiconductors are grown by exchanging two types of MBE chamber.

Our recent activity on nitrides focuses on the initial growth dynamics of nitride films on two-dimensional materials [11]. We used in situ X-ray diffraction (XRD) to investigate the MBE growth of GaN films on graphene-covered SiO_2substrates. As shown in Fig.4, when the AlN buffer layers were deposited before GaN growth, both the lattice parameters of AlN and GaN changed during GaN growth, indicating that AlN acts as a seed for GaN growth. Furthermore, GaN preferred to have an epitaxial relationship with graphene, demonstrating that even ML graphene can be a template for GaN growth. We also confirmed that GaN on graphene can be exfoliated mechanically. GaN growth on graphene-covered

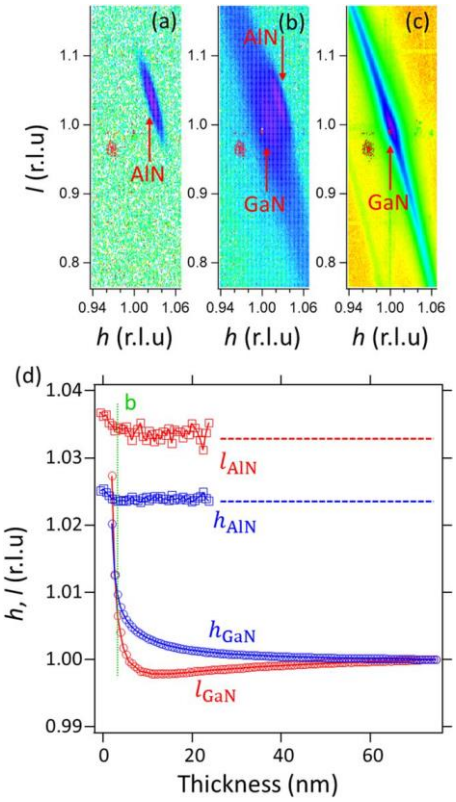

Fig. 4. Reciprocal space maps measured (a) before and (b), (c) during GaN growth on graphene-covered SiO_2 substrate with AlN buffer layers. GaN thicknesses were (b) 3.2 and (c) 74.8 nm. (d) Dependence of XRD spot positions of AlN and GaN on GaN thickness.

SiO_2 can lead to the fabrication of freestanding GaN films by mechanical exfoliation, and it will be useful for flexible photonics/electronics applications.

Takaya Mitsui[*1], Kenji Ishii[*1], Toshiya Inami[*1] and Takuo Sasaki[*2]

[*1] Magnetism Research Group, National Institutes for Quantum and Radiological Science and Technology

[*2] Coherent X-ray Research Group, National Institutes for Quantum and Radiological Science and Technology

References:

[1] Wang, C. S.et al. (1981). *Phys. Rev. B***24**, 4364.

[2] Ohnishi, S. et al. (1983). *Phys. Rev. B***28**, 6741.

[3] Mitsui, T. et al. (2020). *Phys. Rev. Lett.***125**, 236806.

[4] Takayama, T. et al. (2020). *Phys. Rev. Mater.***4**, 075002.

[5] Ishii, K.et al. (2020). *Phys. Rev. Mater.* **5**, 024083.

[6] Pelliciari, J. et al. (2021). *Appl. Phys. Lett.* **118**, 112604.

[7] Inami, T. (2017). *Phys. Rev. Lett.* **119**, 137203.

[8] Sugawara, K. et al. (2021). *J. Appl. Phys.***130**, 113901.

[9] Takahashi, M. (2013). *J. Phys. Soc. Jpn.* **82**, 021011.

[10] Sasaki, T. et al. (2016). *Jpn. J. Appl. Phys.* **55**, 05FB05.

[11] Fuke, S. et al. (2020). *Jpn. J. Appl. Phys.* **59**, 070902.